Limits on the heralding efficiencies and spectral purities of spectrally filtered single photons from photon-pair sources

Evan Meyer-Scott,[*] Nicola Montaut, Johannes Tiedau, Linda Sansoni, Harald Herrmann,
Tim J. Bartley, and Christine Silberhorn

Integrated Quantum Optics, Department of Physics, University of Paderborn, Warburger Straße 100, 33098 Paderborn, Germany

Photon pairs produced by parametric down-conversion or four-wave mixing can interfere with each other in multiport interferometers or carry entanglement between distant nodes for use in entanglement swapping. This requires the photons to be spectrally pure to ensure good interference and have high heralding efficiency to know accurately the number of photons involved and to maintain high rates as the number of photons grows. Spectral filtering is often used to remove noise and define spectral properties. For heralded single photons high purity and heralding efficiency are possible by filtering the heralding arm, but when both photons in typical pair sources are filtered, we show that the heralding efficiency of one or both of the photons is strongly reduced even by ideal spectral filters with 100% transmission in the passband: any improvement in reduced-state spectral purity from filtering comes at the cost of lowered heralding efficiency. We consider the fidelity to a pure, lossless single photon, symmetrize it to include both photons of the pair, and show this quantity is intrinsically limited for sources with spectral correlation. We then provide a framework for this effect for benchmarking common photon-pair sources and present an experiment where we vary the photon filter bandwidths and measure the increase in purity and corresponding reduction in heralding efficiency.

Introduction. Photon pairs from nonlinear optics are so far the only resource to have distributed quantum entanglement over more than a few kilometers [1–6], a critical link in future quantum networks, and are well suited for use in multiport quantum interferometers for sensing, simulation, and computation, both as pairs directly and for heralded single photons [7–10]. Entangled photon pairs have also been used in quantum teleportation [11–13] and entanglement swapping [14–16]. These applications require that the reduced spectral state of each photon is pure: mixedness of the photon states leads to reduced visibility of the interference of independent photons and therefore lower-quality final states.

Parametric down-conversion (PDC) and four-wave mixing (FWM) are the most common sources of photon pairs, and these photons usually possess spectral anticorrelation, leading to mixedness of the reduced state of each photon. This frequency entanglement can be useful for some applications [17] but is catastrophic for multiphoton interference or entanglement-swapping experiments. A convenient solution is narrowband filtering of both photons, which casts each into a single spectral mode, removing entanglement in favor of the spectral purity of each photon. Both FWM sources [13,18–21] and PDC sources [12,22–26] often use filters much narrower than the photon bandwidths. But is spectral filtering compatible also with high *pair-symmetric heralding efficiency* (PSHE), defined as the product of signal and idler heralding efficiencies? In contrast to heralded single-photon sources where only one photon requires high heralding efficiency, we consider photon-pair sources where both photons must be generated in spectrally pure states and with high efficiency, such that both may be used for interference experiments. High heralding efficiency is critical for scaling experiments

and communications to many photons and higher rates [24,25,27] due to the exponential increase in losses with number of photons and also of fundamental importance for reaching scalability in optical quantum computing [28–30], in device-independent quantum cryptography [31,32], and for tests of local causality with entangled photons [33,34]. Our results are especially important for applications that require both high pair-symmetric heralding efficiency and multisource interference: interference of pair sources to produce large entangled states [24,27,35], entanglement swapping [6,14–16,36], heralded noiseless qubit amplification [37,38], quantum repeater networks [39–41], and certain multiphoton phase-estimation schemes [42,43].

Here we show that, for photon-pair sources with spectral correlation or anticorrelation, increasing the spectral purity by filtering comes at a direct cost of decreasing the pair-symmetric heralding efficiency. This trade-off is based only on the joint spectral intensity (JSI) of the photons, not on the underlying physics that produce a specific JSI, meaning our results are applicable to both PDC and FWM and to pulsed and continuous-wave pumps. We find a significant drop in achievable PSHE even with ideal filters. We quantify this trade-off by introducing the symmetrized fidelity of the photon pairs to two spectrally pure single photons and show that it is bounded well below 1 for spectrally correlated sources. This is supported by an experiment using a lithium niobate photon-pair source, where we vary filter parameters and find that heralding efficiency necessarily decreases as purity increases. Similar results could be obtained for spatial correlation and spatial filtering, but here we focus on a single spatial mode.

Previous investigations of filtering in PDC and FWM have largely focused on heralded single photons, where the heralding photon is strongly filtered and the heralded photon is unfiltered, allowing both high spectral purity and

---

*evan.meyer.scott@upb.de

061803-1

high single-sided heralding efficiency [44–46]. The effect of filtering on continuous-variable photon states has been studied [47], as has the effect of self- and cross-phase modulation on filtered photon pairs [48]. Recent theoretical work has included also spatial entanglement and purity with spatial and spectral filters [49], showing again high single-sided heralding efficiency and purity. This is in contrast to source engineering methods, which achieve intrinsically pure states by controlling the dispersion and pump bandwidth [50–63]. Some schemes with tight spectral and time filtering can even outperform this source engineering when considering production rates as well as purity [64,65]. Furthermore, in contrast to spectral filtering after generation, placing the nonlinear medium in a cavity of carefully engineered length and finesse can, in principle, produce spectrally pure states without loss of heralding efficiency [66,67]. In most cases, however, filters are still needed for single-mode operation, as the phase-matching bandwidth covers multiple longitudinal modes of the cavity [45,68–71]; fortunately, for narrowband pumps and filters, these modes do not contribute to a decrease in heralding efficiency because each filter intersects just one cavity mode. For the case where both photons are to be used from nonengineered and noncavity sources, hints that filtering is incompatible with high PSHE have appeared numerous times [50–52,72], and a simple model for heralding efficiency after filtering was developed in [73], but so far no experiments have directly studied the impact of filtering on purity and heralding efficiency simultaneously, and no previous studies have found the fundamental limits to symmetrized fidelity we present here.

Spectrally filtered photon pairs. One can get a feeling for the intrinsic trade-off between reduced-state spectral purity and heralding efficiency from Fig. 1. It shows the joint spectral intensity of an example photon-pair state, overlaid with narrowband filters on each photon, labeled signal and idler. To achieve a spectrally pure state, the JSI that remains after filtering must be uncorrelated between the two photons, either a circle or an ellipse along the vertical or horizontal axis. But for high PSHE, the two-photon amplitudes transmitted by each filter individually must overlap; otherwise, signal photons will pass the filter without the corresponding idler and vice versa.

An uncorrelated JSI, fully contained within both filters, is possible only for certain ranges of the phase-matching angle, namely, $\theta \in [90°, 180°]$, and with a pump bandwidth optimized for the phase-matching bandwidth. But these conditions are precisely those for which filtering is not required since there are no underlying spectral correlations in this condition. Furthermore, achieving a phase-matching angle in this range is nontrivial, as it requires the group velocity of the pump to be between that of the signal and idler. This source engineering is possible [74] only in PDC for very specific wavelength ranges in birefringent crystals [53,75,76]. It is easier to arrange in FWM since it occurs naturally for normal dispersion with the pump between the signal and idler frequencies (here the frequencies are rather close, necessitating narrow filtering for pump removal) or by pumping near the zero-dispersion wavelength [77,78] or using birefringent fibers [79].

As a concrete example we consider waveguided type-II PDC wherein the photons are emitted in a single spatial mode
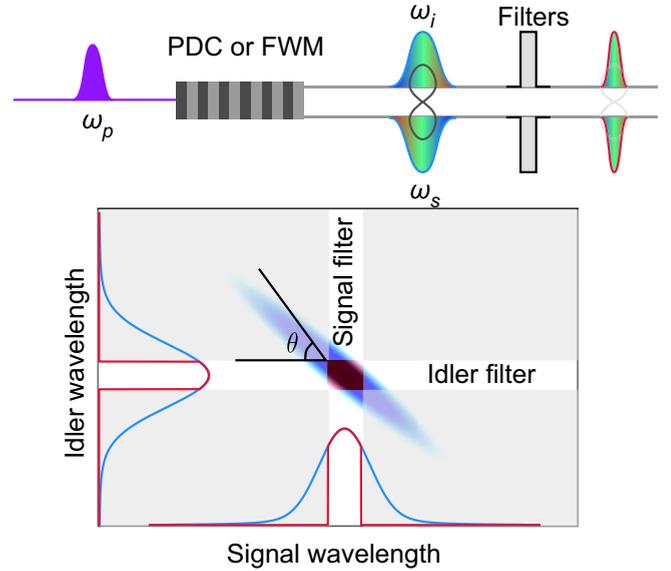

FIG. 1. Photon-pair production and filtering (top), resulting in joint spectral intensity with spectral correlation between signal and idler photons (bottom). The signal and idler filters are overlaid, and the JSI and marginal photon spectra remaining after filtering dictate the reduced-state spectral purity and heralding efficiency of the photons. The phase-matching function with angle θ is multiplied by the pump envelope (which always has an angle of 45°) to produce the total JSI. Thus the overall angle of the JSI is somewhere between 45° and θ.

(such that spatial variables do not play a role) but with different polarizations. These sources can be easily transformed to entangled-pair sources with Sagnac [80] or Mach-Zehnder [81] interferometers. At low enough pump powers to stay in the single-pair regime, the spectral properties of PDC are governed by the joint spectral amplitude $f(\omega_s, \omega_i)$ for signal and idler frequencies ω_s and ω_i, giving rise to the photon-pair state [50]

$$|\psi\rangle = \iint d\omega_s d\omega_i \, f(\omega_s, \omega_i) \mathcal{F}_s(\omega_s) \mathcal{F}_i(\omega_i) |\omega_s\rangle |\omega_i\rangle, \quad (1)$$

where $|\omega_s\rangle$ and $|\omega_i\rangle$ are single photons at frequency ω_s and ω_i with the polarization of the signal or idler mode and $\mathcal{F}_s(\omega_s)$ and $\mathcal{F}_i(\omega_i)$ are spectral filters on the signal and idler photons, respectively. The joint spectral intensity is $|f(\omega_s, \omega_i) \mathcal{F}_s(\omega_s) \mathcal{F}_i(\omega_i)|^2$, and the filters can be of any shape: we consider square and Gaussian filters.

We model the joint spectral amplitude around central frequencies ω_{s0} and ω_{i0} by

$$f(\omega_s, \omega_i)$$
$$= N \exp\left(\frac{-(\omega_s - \omega_{s0} + \omega_i - \omega_{i0})^2}{4\sigma_p^2} \right)$$
$$\times \text{sinc}\left(\frac{([\omega_s - \omega_{s0}] \sin\theta + [\omega_i - \omega_{i0}] \cos\theta)}{2\sigma_{pm}} \right). \quad (2)$$

The pump and phase-matching bandwidths are σ_p and σ_{pm}, respectively; N is a normalization term; and the phase-matching angle [79] is $\theta = \arctan\left(\frac{k_p' - k_s'}{k_p' - k_i'}\right)$, where k_x' is the frequency derivative of the wave number k of mode x. Thus the nonlinear

material, waveguide characteristics, and wavelengths can all be chosen to determine the phase-matching angle.

Heralding efficiency and reduced-state spectral purity. We define the signal photon's *filter heralding efficiency* as the probability that the signal photon passes its filter given that the idler photon has passed its filter and vice versa for the idler photon's filter heralding efficiency. These efficiencies will be less than 1 whenever the JSIs passed by each filter individually do not match [49,73]. Defining the probability that both photons pass their filters as Γ_{both} and the probability that each passes individually as Γ_s and Γ_i, we find the signal's filter heralding efficiency is $\eta_{f,s} = \frac{\Gamma_{\text{both}}}{\Gamma_i}$ and the idler's is $\eta_{f,i} = \frac{\Gamma_{\text{both}}}{\Gamma_s}$. Then we define the pair-symmetric heralding efficiency as $\eta_{f,s}\eta_{f,i}$. Of course this is only the contribution of filtering to the PSHE; optical losses will lower the PSHE further.

The spectral purity of the reduced state of either photon given that both photons have passed their respective filters (corresponding to the relevant case of coincident detection) is [82] $P = \text{Tr}(\rho_s^2)$, where

$$\rho_s = \text{Tr}_i(|\psi\rangle\langle\psi|)$$

$$= \iiint d\omega_i d\omega_s d\omega_s' f(\omega_s,\omega_i) f^*(\omega_s',\omega_i)$$

$$\times \mathcal{F}_s(\omega_s)\mathcal{F}_s(\omega_s')\mathcal{F}_i(\omega_i)^2 |\omega_s\rangle\langle\omega_s'| \qquad (3)$$

is the reduced density matrix. The purity can be taken for either signal or idler as there is no other degree of freedom (e.g., spatial) that would allow different purities for each mode and we always consider that the photons are detected in coincidence.

Taking the JSI of Fig. 1 (with a pump bandwidth of 0.42 nm, a phase-matching bandwidth of 0.46 nm, and $\theta = 60.5°$, matching the experiment below), we calculate the filter heralding efficiencies and spectral purity versus filter bandwidth, which are taken to be equal for the signal and idler. As seen in Fig. 2, as soon as the filters are narrow enough to increase the purity, the filter heralding efficiency starts to drop. The filters are ideal flat-top filters with perfect transmission in the passband and perfect blocking otherwise. This is an idealization of real dense-wave-division multiplexing filters, chosen to highlight the intrinsic physical effects of filtering rather than the technical effects. In fact, real filters lead to even stronger reductions in heralding efficiency due to nonuniformities, slow roll-off, and nonunit transmission. Gaussian filters (thin gray curves) show worse performance for both purity and heralding efficiency, with the improved purity at large filter bandwidths due to the removal of sinc lobes under the Gaussian approximation of the JSI. The kink in Fig. 2 around 3-nm filter bandwidth in the idler heralding efficiency is due to the asymmetry of the JSI [83]. Even though both filters are varied equally, since the JSI is tipped slightly towards parallel to the idler axis, above the kink, the filtering is dominated by the idler filter, while below both filters contribute.

To quantify the combined effect of filtering on heralding efficiency and purity we introduce the symmetrized fidelity $F = \sqrt{F_s F_i}$, where F_j is the fidelity for the signal or idler to a pure single photon state $|1\rangle_j = \int d\omega g_j(\omega)(\hat{a})_j^\dagger(\omega)|0\rangle$ after heralding by the idler or signal and including the vacuum
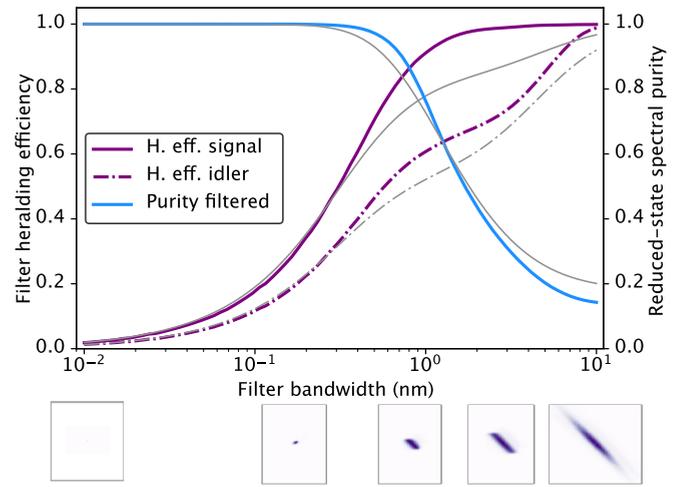

FIG. 2. Theoretical filter heralding efficiency for signal (purple solid line) and idler (purple dashed line), combined PSHE (purple dotted line), and spectral purity (blue line) versus filter bandwidth for the flat-top filters with the same bandwidth for signal and idler, showing the intrinsic trade-off between purity and efficiency. The corresponding thin gray curves are the analytic results for Gaussian filters. Some representative JSIs are shown below their corresponding filter bandwidths (the leftmost is very small on this scale).

component caused by filtering losses. We symmetrize the fidelity in this way rather than taking just the signal or idler fidelity to capture the effects of filtering on both photons together. The spectral function $g(\omega)$ is optimized for each photon to maximize the fidelity, as it is not directly given by any eigenvector of the reduced density matrix Eq. (3). The individual fidelities are

$$F_s = \eta_{f,s} \max_{g_s(\omega)} \langle 1|_s \, \rho_s \, |1\rangle_s \,,$$

$$F_i = \eta_{f,i} \max_{g_i(\omega)} \langle 1|_i \, \rho_i \, |1\rangle_i \,. \qquad (4)$$

Either F_s or F_i can be made to approach 1 by filtering but, in general, not both simultaneously. Using the Gaussian approximation developed in the Supplemental Material [84], which allows analytic solutions, we find the symmetrized fidelity to be related to the purity and heralding efficiency by

$$F = \sqrt{\eta_{f,s}\eta_{f,i}} \, \frac{2P}{1+P}. \qquad (5)$$

By optimizing the pump and filter bandwidths for each phase-matching angle we bound the maximum value of symmetrized fidelity available by filtering, as shown in Fig. 3. The maximum is independent of the phase-matching bandwidth (here chosen to be 1.5 nm), although the optimal pump and filter bandwidths change. For our lithium niobate (LN) crystal with $\theta = 60.5°$ the maximum is $F = 0.57$. By contrast, sources with $\theta \in [90°,180°]$ can have $F \to 1$ even without filtering, as the optimal filter bandwidth goes to infinity. This shows clearly the futility of filtering for reduced-state spectral purity in PDC: the conditions in which filters are needed are only where filtering cannot recover perfect fidelity due to lowered heralding efficiency. Of course without filters in
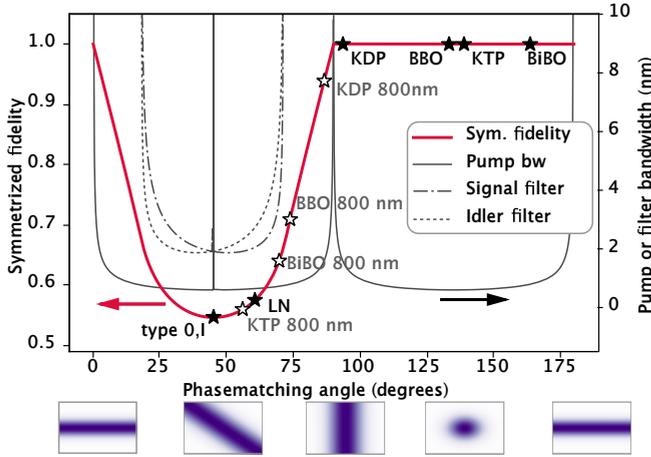
FIG. 3. Calculated symmetrized fidelity $\sqrt{F_s F_i}$ (thick red line) versus phase-matching angle after optimizing the pump bandwidth (black solid line) and the signal (black dot-dashed line) and idler (black dashed line) filter bandwidths. The maximum achievable fidelity is independent of the crystal length, but the optimal values of bandwidth change to accommodate the different phase-matching bandwidths. A few crystal types [85] for degenerate type-II PDC to 1550 nm are overlaid (solid stars), while for degenerate type-0 and type-I bandwidths, the phase-matching angle is always 45° (except with engineered dispersion, for example, in microstructured fibers [54] or for noncollinear PDC [27]). With nondegenerate photons and other wavelengths (see three examples at 800 nm, open stars) many different angles can be reached [76]. Below the plot are unfiltered JSIs at 45° intervals.

these conditions the fidelity to a pure single photon would be even lower. We stress that this fidelity bound is generic for all PDC and FWM sources (with JSIs described by the pump-times-phase-matching model) and is thus a very powerful tool in source design.

Finally, to show the sharpness of these effects we vary the filter bandwidths independently and set the pump and phase-matching bandwidths to 0.38 and 1.5 nm, respectively, which for $\theta = 60.5°$ allows an optimal symmetrized fidelity. As shown in Fig. 4, the best filter heralding efficiencies for the signal photon have the largest signal filter and the smallest idler filter and vice versa for the idler photon. However, the largest purity requires small filters on both arms, resulting in a symmetrized fidelity that varies slowly over filter bandwidth and never exceeds 0.57, falling to zero as either filter gets too narrow.

Experiment. To confirm the trade-off between purity and PSHE, we measured the heralding efficiency of signal and idler photons and the joint spectral intensities of a photon-pair source under various filtering conditions. The source (Fig. 1) was a 21-mm type-II periodically poled lithium niobate waveguide, fiber pigtailed on both ends [86] and pumped by a Ti:sapphire pulsed laser with a wavelength of 778 nm. The laser had a pulse width of 3.0 ps FWHM, nearly transform limited to 0.42-nm FWHM spectral bandwidth, and 5-μW coupled power, resulting in a production of $\sim$0.02 pair/pulse before filtering. Calculations for lithium niobate predict a phase-matching angle of 60.5° and a bandwidth of 0.46 nm. The output of the source was coupled to a WaveShaper 4000
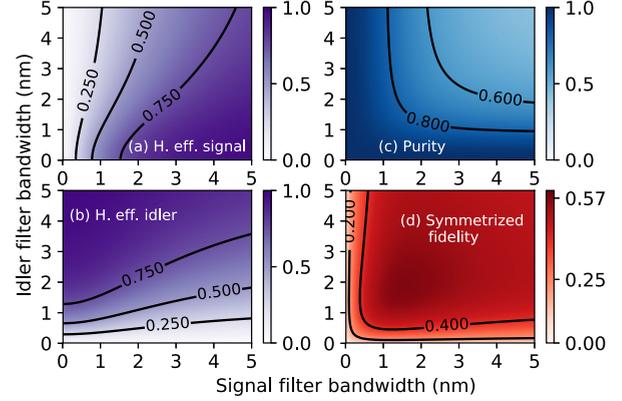

FIG. 4. Filter heralding efficiencies for (a) signal and (b) idler as a function of signal and idler filter bandwidths, along with (c) reduced-state spectral purity and (d) symmetrized fidelity to a spectrally pure single photon. Here we use Gaussian filters, with bandwidths given by the FWHM. While the heralding efficiencies and purity range individually over [0,1], the symmetrized fidelity is reasonably constant around its mean value of 0.45 and never surpasses 0.57.

(Finisar Corp.) which was used to separate the nondegenerate photons (central wavelengths of 1562 and 1549 nm) and define their spectral filters.

We characterize the heralding efficiency for each filter setting using the Klyshko method [87] such that $\eta_s = \frac{C}{S_i}$, $\eta_i = \frac{C}{S_s}$, where C are the number of coincidences, S_s and S_i are the number of signal and idler singles, respectively, and η_s and η_i are the total heralding efficiencies. Then we extract the filter heralding efficiency by dividing out the heralding efficiency $\eta_{\max,s}$ or $\eta_{\max,i}$ when the filters are set to maximum bandwidth, which comes from nonunit coupling and detector efficiencies. Thus the filter heralding efficiencies are

$$\eta_{f,s} = \frac{C}{S_i \eta_{\max,s}}, \eta_{f,i} = \frac{C}{S_s \eta_{\max,i}}. \quad (6)$$

We confirmed that the peak filter transmission is independent of the WaveShaper's filter bandwidth assuring that the reduction in heralding efficiency is due to the fundamental trade-off rather than technical imperfections (see plot in Supplemental Material [84]).

We characterized the purity by measuring a joint spectral intensity with a time-of-flight spectrometer [88], assuming a constant phase of the joint spectrum [58] and calculating $P = \text{Tr}(\rho_a^2)$, where ρ_a is the reduced spectral density matrix of the signal or idler photon [82]. Using the JSI as an indicator of purity can be limited by artificial smoothing from limited spectrometer resolution and spectral phases that are not identifiable with intensity measurements. Thus we have employed as high a resolution as possible and verified numerically that the expected phases due to pump chirp are negligible. We show in Fig. 5 the joint spectral intensities after filtering and the corresponding purities, calculated with an additional time filter of twice the filter bandwidth to reduce technical noise from our laser's instability and the limited timing resolution of our spectrometer.
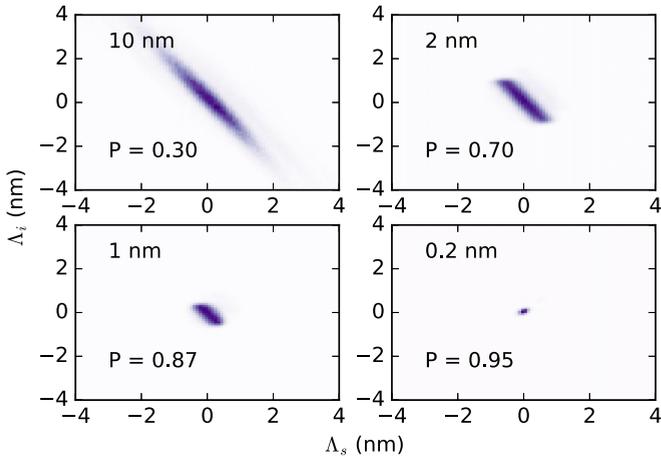
FIG. 5. Measured joint spectral intensities of photon pairs, from nearly unfiltered (10-nm bandwidth) to strongly filtered and spectrally pure (0.2-nm bandwidth). The axis labels Λ give the distance from the central wavelength.
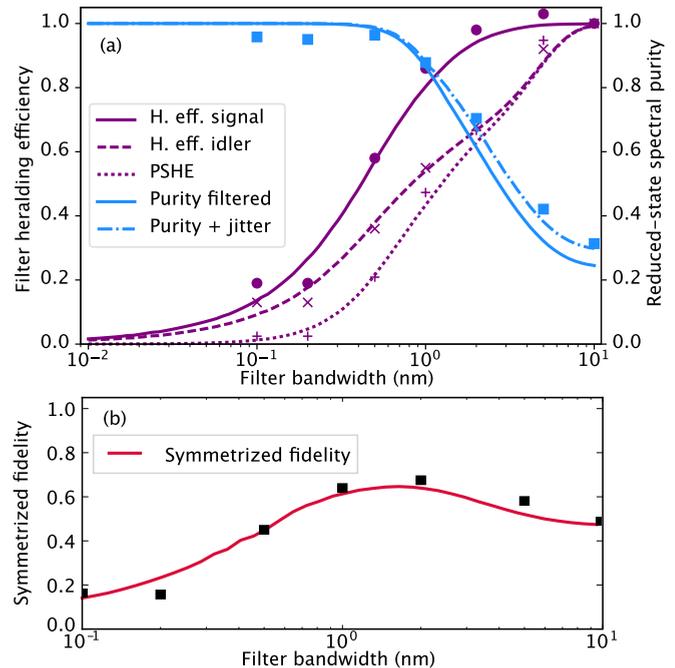

FIG. 6. (a) Experimental filter heralding efficiency, PSHE, and spectral purity and (b) symmetrized fidelity versus filter bandwidth (points), with theoretical prediction (curves). The experimental data are shown with error bars from Poissonian statistics smaller than symbol size. Adding artificial jitter to the theoretical JSI makes the purity agree with the experiment for large filters, and thus this jitter has also been applied to the theoretical calculation for symmetrized fidelity.

The purity, filter heralding efficiencies, and symmetrized fidelity are plotted in Fig. 6 and correspond reasonably well to the predictions after accounting for the asymmetry of our measured JSI. The limited resolution of our fiber spectrometer due to detector timing jitter tends to increase measured purities for large filters, as it rounds off sharp features of the JSI. Adding our experimental detector timing jitter of 120 ps to the theoretical JSI makes the predicted purity match the experiment for large filters. The remaining mismatch in the symmetrized fidelity could be due to small ripples in the WaveShaper transmission. The overall trend is clear: the increase in purity comes at a direct cost of heralding efficiency, and the fidelity of the signal and idler states to pure single photons cannot reach unity by filtering.

Conclusion. We have shown that spectral filtering of down-converted photons to increase the reduced-state spectral purity can lead to intrinsically low pair-symmetric heralding efficiencies and cannot increase the symmetrized fidelity to a pure single photon beyond strong, general bounds. Our results suggest that, if high heralding efficiency of photon pairs is important, source engineering is required to generate spectrally decorrelated states, and for noise reduction only broadband filters should be used. The problem of reduced efficiency could also be avoided with carefully designed cavities [68] or more general time-frequency filtering [64] to directly select single spectral-temporal modes [89].

For example, without the reduction of heralding efficiency from narrowband filtering, the rate of ten-photon entanglement in two recent experiments [24,25] could have been increased by a factor of 10 (counting only the reduction of heralding efficiencies) or a factor 100 (counting all filtering losses). For heralded photon sources, care must be taken when filtering the heralded photon so as not to decrease its heralding efficiency unnecessarily. Finally, the analytic expressions we developed [84] will be useful in designing the next generation of photon-pair sources, as they allow optimization of the spectral purity and heralding efficiency with and without filtering. It would be interesting in future work to design the optimal filter shape that minimizes the purity-efficiency trade-off or maximizes the symmetrized fidelity.

[1] R. Ursin, F. Tiefenbacher, T. Schmitt-Manderbach, H. Weier, T. Scheidl, M. Lindenthal, B. Blauensteiner, T. Jennewein, J. Perdigues, P. Trojek, B. Oemer, M. Fuerst, M. Meyenburg, J. Rarity, Z. Sodnik, C. Barbieri, H. Weinfurter, and A. Zeilinger, Free-space distribution of entanglement and single photons over 144 km, Nat. Phys. **3**, 481 (2007).

[2] T. Scheidl, R. Ursin, A. Fedrizzi, S. Ramelow, X.-S. Ma, T. Herbst, R. Prevedel, L. Ratschbacher, J. Kofler, T. Jennewein,

and A. Zeilinger, Feasibility of 300 km quantum key distribution with entangled states, New J. Phys. **11**, 085002 (2009).

[3] J. F. Dynes, H. Takesue, Z. L. Yuan, A. W. Sharpe, K. Harada, T. Honjo, H. Kamada, O. Tadanaga, Y. Nishida, M. Asobe, and A. J. Shields, Efficient entanglement distribution over 200 kilometres, Opt. Express **17**, 11440 (2009).

[4] T. Inagaki, N. Matsuda, O. Tadanaga, M. Asobe, and H. Takesue, Entanglement distribution over 300 km of fiber, Opt. Express **21**, 23241 (2013).

[5] X.-S. Ma, T. Herbst, T. Scheidl, D. Wang, S. Kropatschek, W. Naylor, B. Wittmann, A. Mech, J. Kofler, E. Anisimova, V. Makarov, T. Jennewein, R. Ursin, and A. Zeilinger, Quantum teleportation over 143 kilometres using active feed-forward, Nature (London) **489**, 269 (2012).

[6] T. Herbst, T. Scheidl, M. Fink, J. Handsteiner, B. Wittmann, R. Ursin, and A. Zeilinger, Teleportation of entanglement over 143 km, Proc. Natl. Acad. Sci. USA **112**, 14202 (2015).

[7] B. J. Metcalf, N. Thomas-Peter, J. B. Spring, D. Kundys, M. A. Broome, P. C. Humphreys, X.-M. Jin, M. Barbieri, W. S. Kolthammer, J. C. Gates, B. J. Smith, N. K. Langford, P. G. R. Smith, and I. A. Walmsley, Multiphoton quantum interference in a multiport integrated photonic device, Nat. Commun. **4**, 1356 (2013).

[8] A. Crespi, R. Osellame, R. Ramponi, D. J. Brod, E. F. Galvao, N. Spagnolo, C. Vitelli, E. Maiorino, P. Mataloni, and F. Sciarrino, Integrated multimode interferometers with arbitrary designs for photonic boson sampling, Nat. Photonics **7**, 545 (2013).

[9] M. Tillmann, B. Dakic, R. Heilmann, S. Nolte, A. Szameit, and P. Walther, Experimental boson sampling, Nat. Photonics **7**, 540 (2013).

[10] J. Carolan, C. Harrold, C. Sparrow, E. Martín-López, N. J. Russell, J. W. Silverstone, P. J. Shadbolt, N. Matsuda, M. Oguma, M. Itoh, G. D. Marshall, M. G. Thompson, J. C. F. Matthews, T. Hashimoto, J. L. O'Brien, and A. Laing, Universal linear optics, Science **349**, 711 (2015).

[11] H. Takesue, S. D. Dyer, M. J. Stevens, V. Verma, R. P. Mirin, and S. W. Nam, Quantum teleportation over 100 km of fiber using highly efficient superconducting nanowire single-photon detectors, Optica **2**, 832 (2015).

[12] R. Valivarthi, M. G. Puigibert, Q. Zhou, G. H. Aguilar, V. B. Verma, F. Marsili, M. D. Shaw, S. W. Nam, D. Oblak, and W. Tittel, Quantum teleportation across a metropolitan fibre network, Nat. Photonics **10**, 676 (2016).

[13] Q.-C. Sun, Y.-L. Mao, S.-J. Chen, W. Zhang, Y.-F. Jiang, Y.-B. Zhang, W.-J. Zhang, S. Miki, T. Yamashita, H. Terai, X. Jiang, T.-Y. Chen, L.-X. You, X.-F. Chen, Z. Wang, J.-Y. Fan, Q. Zhang, and J.-W. Pan, Quantum teleportation with independent sources and prior entanglement distribution over a network, Nat. Photonics **10**, 671 (2016).

[14] H. Takesue and B. Miquel, Entanglement swapping using telecom-band photons generated in fibers, Opt. Express **17**, 10748 (2009).

[15] Y. Xue, A. Yoshizawa, and H. Tsuchida, Polarization-based entanglement swapping at the telecommunication wavelength using spontaneous parametric down-conversion photon-pair sources, Phys. Rev. A **85**, 032337 (2012).

[16] R.-B. Jin, M. Takeoka, U. Takagi, R. Shimizu, and M. Sasaki, Highly efficient entanglement swapping and teleportation at telecom wavelength, Sci. Rep. **5**, 9333 (2015).

[17] A. F. Abouraddy, M. B. Nasr, B. E. A. Saleh, A. V. Sergienko, and M. C. Teich, Quantum-optical coherence tomography with dispersion cancellation, Phys. Rev. A **65**, 053817 (2002).

[18] J. E. Sharping, K. F. Lee, M. A. Foster, A. C. Turner, B. S. Schmidt, M. Lipson, A. L. Gaeta, and P. Kumar, Generation of correlated photons in nanoscale silicon waveguides, Opt. Express **14**, 12388 (2006).

[19] K.-i. Harada, H. Takesue, H. Fukuda, T. Tsuchizawa, T. Watanabe, K. Yamada, Y. Tokura, and S.-i. Itabashi, Indistinguishable photon pair generation using two independent silicon wire waveguides, New J. Phys. **13**, 065005 (2011).

[20] C. Xiong, G. D. Marshall, A. Peruzzo, M. Lobino, A. S. Clark, D.-Y. Choi, S. J. Madden, C. M. Natarajan, M. G. Tanner, R. H. Hadfield, S. N. Dorenbos, T. Zijlstra, V. Zwiller, M. G. Thompson, J. G. Rarity, M. J. Steel, B. Luther-Davies, B. J. Eggleton, and J. L. O'Brien, Generation of correlated photon pairs in a chalcogenide As$_2$S$_3$ waveguide, Appl. Phys. Lett. **98**, 051101 (2011).

[21] J. W. Silverstone, D. Bonneau, K. Ohira, N. Suzuki, H. Yoshida, N. Iizuka, M. Ezaki, C. M. Natarajan, M. G. Tanner, R. H. Hadfield, V. Zwiller, G. D. Marshall, J. G. Rarity, J. L. O'Brien, and M. G. Thompson, On-chip quantum interference between silicon photon-pair sources, Nat. Photonics **8**, 104 (2013).

[22] P. Aboussouan, O. Alibart, D. B. Ostrowsky, P. Baldi, and S. Tanzilli, High-visibility two-photon interference at a telecom wavelength using picosecond-regime separated sources, Phys. Rev. A **81**, 021801 (2010).

[23] N. Bruno, E. Zambrini Cruzeiro, A. Martin, and R. T. Thew, Simple, pulsed, polarization entangled photon pair source, Opt. Commun. **327**, 3 (2014).

[24] X.-L. Wang, L.-K. Chen, W. Li, H.-L. Huang, C. Liu, C. Chen, Y.-H. Luo, Z.-E. Su, D. Wu, Z.-D. Li, H. Lu, Y. Hu, X. Jiang, C.-Z. Peng, L. Li, N.-L. Liu, Y.-A. Chen, C.-Y. Lu, and J.-W. Pan, Experimental Ten-Photon Entanglement, Phys. Rev. Lett. **117**, 210502 (2016).

[25] L.-K. Chen, Z.-D. Li, X.-C. Yao, M. Huang, W. Li, H. Lu, X. Yuan, Y.-B. Zhang, X. Jiang, C.-Z. Peng, L. Li, N.-L. Liu, X. Ma, C.-Y. Lu, Y.-A. Chen, and J.-W. Pan, Observation of ten-photon entanglement using thin BiB$_3$O$_6$ crystals, Optica **4**, 77 (2017).

[26] P. Vergyris, T. Meany, T. Lunghi, G. Sauder, J. Downes, M. J. Steel, M. J. Withford, O. Alibart, and S. Tanzilli, On-chip generation of heralded photon-number states, Sci. Rep. **6**, 35975 (2016).

[27] L. E. Vicent, A. B. U'Ren, R. Rangarajan, C. I. Osorio, J. P. Torres, L. Zhang, and I. A. Walmsley, Design of bright, fiber-coupled and fully factorable photon pair sources, New J. Phys. **12**, 093027 (2010).

[28] M. Varnava, D. E. Browne, and T. Rudolph, How Good Must Single Photon Sources and Detectors be for Efficient Linear Optical Quantum Computation? Phys. Rev. Lett. **100**, 060502 (2008).

[29] Y.-X. Gong, X.-B. Zou, T. C. Ralph, S.-N. Zhu, and G.-C. Guo, Linear optical quantum computation with imperfect entangled photon-pair sources and inefficient non-photon-number-resolving detectors, Phys. Rev. A **81**, 052303 (2010).

[30] T. Jennewein, M. Barbieri, and A. G. White, Single-photon device requirements for operating linear optics quantum computing outside the post-selection basis, J. Mod. Opt. **58**, 276 (2011).

[31] A. Acín, N. Brunner, N. Gisin, S. Massar, S. Pironio, and V. Scarani, Device-Independent Security of Quantum Cryptography Against Collective Attacks, Phys. Rev. Lett. **98**, 230501 (2007).

[32] M. Lucamarini, G. Vallone, I. Gianani, P. Mataloni, and G. Di Giuseppe, Device-independent entanglement-based Bennett 1992 protocol, Phys. Rev. A **86**, 032325 (2012).

[33] M. Giustina, M. A. M. Versteegh, S. Wengerowsky, J. Handsteiner, A. Hochrainer, K. Phelan, F. Steinlechner, J. Kofler, J.-A. Larsson, C. Abellán, W. Amaya, V. Pruneri, M. W. Mitchell, J. Beyer, T. Gerrits, A. E. Lita, L. K. Shalm, S. W. Nam, T. Scheidl, R. Ursin, B. Wittmann, and A. Zeilinger, Significant-Loophole-Free Test of Bell's Theorem with Entangled Photons, Phys. Rev. Lett. **115**, 250401 (2015).

[34] L. K. Shalm, E. Meyer-Scott, B. G. Christensen, P. Bierhorst, M. A. Wayne, M. J. Stevens, T. Gerrits, S. Glancy, D. R. Hamel, M. S. Allman, K. J. Coakley, S. D. Dyer, C. Hodge, A. E. Lita, V. B. Verma, C. Lambrocco, E. Tortorici, A. L. Migdall, Y. Zhang, D. R. Kumor, W. H. Farr, F. Marsili, M. D. Shaw, J. A. Stern, C. Abellán, W. Amaya, V. Pruneri, T. Jennewein, M. W. Mitchell, P. G. Kwiat, J. C. Bienfang, R. P. Mirin, E. Knill, and S. W. Nam, Strong Loophole-Free Test of Local Realism, Phys. Rev. Lett. **115**, 250402 (2015).

[35] J.-W. Pan, D. Bouwmeester, M. Daniell, H. Weinfurter, and A. Zeilinger, Experimental test of quantum nonlocality in three-photon Greenberger-Horne-Zeilinger entanglement, Nature (London) **403**, 515 (2000).

[36] J.-W. Pan, D. Bouwmeester, H. Weinfurter, and A. Zeilinger, Experimental Entanglement Swapping: Entangling Photons that Never Interacted, Phys. Rev. Lett. **80**, 3891 (1998).

[37] S. Kocsis, G. Y. Xiang, T. C. Ralph, and G. J. Pryde, Heralded noiseless amplification of a photon polarization qubit, Nat. Phys. **9**, 23 (2013).

[38] N. Bruno, V. Pini, A. Martin, V. B. Verma, S. W. Nam, R. Mirin, A. Lita, F. Marsili, B. Korzh, F. Bussières, N. Sangouard, H. Zbinden, N. Gisin, and R. Thew, Heralded amplification of photonic qubits, Opt. Express **24**, 125 (2016).

[39] K. Azuma, K. Tamaki, and H.-K. Lo, All-photonic quantum repeaters, Nat. Commun. **6**, 6787 (2015).

[40] S. Guha, H. Krovi, C. A. Fuchs, Z. Dutton, J. A. Slater, C. Simon, and W. Tittel, Rate-loss analysis of an efficient quantum repeater architecture, Phys. Rev. A **92**, 022357 (2015).

[41] H. Krovi, S. Guha, Z. Dutton, J. A. Slater, C. Simon, and W. Tittel, Practical quantum repeaters with parametric down-conversion sources, Appl. Phys. B **122**, 52 (2016).

[42] F. W. Sun, B. H. Liu, Y. X. Gong, Y. F. Huang, Z. Y. Ou, and G. C. Guo, Experimental demonstration of phase measurement precision beating standard quantum limit by projection measurement, Europhys. Lett. **82**, 24001 (2008).

[43] G. Y. Xiang, H. F. Hofmann, and G. J. Pryde, Optimal multiphoton phase sensing with a single interference fringe, Sci. Rep. **3**, 2684 (2013).

[44] T. Aichele, A. I. Lvovsky, and S. Schiller, Optical mode characterization of single photons prepared by means of conditional measurements on a biphoton state, Eur. Phys. J. D **18**, 237 (2002).

[45] J. S. Neergaard-Nielsen, B. M. Nielsen, H. Takahashi, A. I. Vistnes, and E. S. Polzik, High purity bright single photon source, Opt. Express **15**, 7940 (2007).

[46] A. M. Brańczyk, T. C. Ralph, W. Helwig, and C. Silberhorn, Optimized generation of heralded Fock states using parametric down-conversion, New J. Phys. **12**, 063001 (2010).

[47] A. Christ, C. Lupo, M. Reichelt, T. Meier, and C. Silberhorn, Theory of filtered type-II parametric down-conversion in the continuous-variable domain: Quantifying the impacts of filtering, Phys. Rev. A **90**, 023823 (2014).

[48] G. F. Sinclair and M. G. Thompson, Effect of self- and cross-phase modulation on photon pairs generated by spontaneous four-wave mixing in integrated optical waveguides, Phys. Rev. A **94**, 063855 (2016).

[49] J. Flórez, O. Calderón, A. Valencia, and C. I. Osorio, Correlation control for pure and efficiently generated heralded single photons, Phys. Rev. A **91**, 013819 (2015); Erratum: Correlation control for pure and efficiently generated heralded single photons [Phys. Rev. A **91**, 013819 (2015)] **94**, 069901(E) (2016).

[50] W. P. Grice and I. A. Walmsley, Spectral information and distinguishability in type-II down-conversion with a broadband pump, Phys. Rev. A **56**, 1627 (1997).

[51] W. P. Grice, A. B. U'Ren, and I. A. Walmsley, Eliminating frequency and space-time correlations in multiphoton states, Phys. Rev. A **64**, 063815 (2001).

[52] P. J. Mosley, J. S. Lundeen, B. J. Smith, P. Wasylczyk, A. B. U'Ren, C. Silberhorn, and I. A. Walmsley, Heralded Generation of Ultrafast Single Photons in Pure Quantum States, Phys. Rev. Lett. **100**, 133601 (2008).

[53] A. B. U'Ren, C. Silberhorn, R. Erdmann, K. Banaszek, W. P. Grice, I. A. Walmsley, and M. G. Raymer, Generation of pure-state single-photon wavepackets by conditional preparation based on spontaneous parametric downconversion, Laser Phys. **15**, 146 (2005).

[54] K. Garay-Palmett, H. J. McGuinness, O. Cohen, J. S. Lundeen, R. Rangel-Rojo, A. B. U'ren, M. G. Raymer, C. J. McKinstrie, S. Radic, and I. A. Walmsley, Photon pair-state preparation with tailored spectral properties by spontaneous four-wave mixing in photonic-crystal fiber, Opt. Express **15**, 14870 (2007).

[55] M. Halder, J. Fulconis, B. Cemlyn, A. Clark, C. Xiong, W. J. Wadsworth, and J. G. Rarity, Nonclassical 2-photon interference with separate intrinsically narrowband fibre sources, Opt. Express **17**, 4670 (2009).

[56] Z. H. Levine, J. Fan, J. Chen, A. Ling, and A. Migdall, Heralded, pure-state single-photon source based on a potassium titanyl phosphate waveguide, Opt. Express **18**, 3708 (2010).

[57] A. Eckstein, A. Christ, P. J. Mosley, and C. Silberhorn, Highly Efficient Single-Pass Source of Pulsed Single-Mode Twin Beams of Light, Phys. Rev. Lett. **106**, 013603 (2011).

[58] T. Gerrits, M. J. Stevens, B. Baek, B. Calkins, A. Lita, S. Glancy, E. Knill, S. W. Nam, R. P. Mirin, R. H. Hadfield, R. S. Bennink, W. P. Grice, S. Dorenbos, T. Zijlstra, T. Klapwijk, and V. Zwiller, Generation of degenerate, factorizable, pulsed squeezed light at telecom wavelengths, Opt. Express **19**, 24434 (2011).

[59] B. Fang, O. Cohen, J. B. Moreno, and V. O. Lorenz, State engineering of photon pairs produced through dual-pump spontaneous four-wave mixing, Opt. Express **21**, 2707 (2013).

[60] G. Harder, V. Ansari, B. Brecht, T. Dirmeier, C. Marquardt, and C. Silberhorn, An optimized photon pair source for quantum circuits, Opt. Express **21**, 13975 (2013).

[61] M. Förtsch, J. U. Fürst, C. Wittmann, D. Strekalov, A. Aiello, M. V. Chekhova, C. Silberhorn, G. Leuchs, and C. Marquardt, A versatile source of single photons for quantum information processing, Nat. Commun. **4**, 1818 (2013).

[62] N. Bruno, A. Martin, T. Guerreiro, B. Sanguinetti, and R. T. Thew, Pulsed source of spectrally uncorrelated and indistinguishable photons at telecom wavelengths, Opt. Express **22**, 17246 (2014).

[63] M. M. Weston, H. M. Chrzanowski, S. Wollmann, A. Boston, J. Ho, L. K. Shalm, V. B. Verma, M. S. Allman, S. W. Nam, R. B. Patel, S. Slussarenko, and G. J. Pryde, Efficient and pure femtosecond-pulse-length source of polarization-entangled photons, Opt. Express **24**, 10869 (2016).

[64] Y.-P. Huang, J. B. Altepeter, and P. Kumar, Heralding single photons without spectral factorability, Phys. Rev. A **82**, 043826 (2010).

[65] Y.-P. Huang, J. B. Altepeter, and P. Kumar, Optimized heralding schemes for single photons, Phys. Rev. A **84**, 033844 (2011).

[66] C.-S. Chuu, G. Y. Yin, and S. E. Harris, A miniature ultrabright source of temporally long, narrowband biphotons, Appl. Phys. Lett. **101**, 051108 (2012).

[67] K.-H. Luo, H. Herrmann, S. Krapick, B. Brecht, R. Ricken, V. Quiring, H. Suche, W. Sohler, and C. Silberhorn, Direct generation of genuine single-longitudinal-mode narrowband photon pairs, New J. Phys. **17**, 073039 (2015).

[68] Y. Jeronimo-Moreno, S. Rodriguez-Benavides, and A. B. U'Ren, Theory of cavity-enhanced spontaneous parametric downconversion, Laser Phys. **20**, 1221 (2010).

[69] X.-H. Bao, Y. Qian, J. Yang, H. Zhang, Z.-B. Chen, T. Yang, and J.-W. Pan, Generation of Narrow-Band Polarization-Entangled Photon Pairs for Atomic Quantum Memories, Phys. Rev. Lett. **101**, 190501 (2008).

[70] M. Scholz, L. Koch, and O. Benson, Statistics of Narrow-Band Single Photons for Quantum Memories Generated by Ultrabright Cavity-Enhanced Parametric Down-Conversion, Phys. Rev. Lett. **102**, 063603 (2009).

[71] J. Fekete, D. Rieländer, M. Cristiani, and H. de Riedmatten, Ultranarrow-Band Photon-Pair Source Compatible with Solid State Quantum Memories and Telecommunication Networks, Phys. Rev. Lett. **110**, 220502 (2013).

[72] M. Bock, A. Lenhard, C. Chunnilall, and C. Becher, Highly efficient heralded single-photon source for telecom wavelengths based on a PPLN waveguide, Opt. Express **24**, 23992 (2016).

[73] J. Jin, M. Grimau Puigibert, L. Giner, J. A. Slater, M. R. E. Lamont, V. B. Verma, M. D. Shaw, F. Marsili, S. W. Nam, D. Oblak, and W. Tittel, Entanglement swapping with quantum-memory-compatible photons, Phys. Rev. A **92**, 012329 (2015).

[74] L. Zhang, C. Söller, O. Cohen, B. J. Smith, and I. A. Walmsley, Heralded generation of single photons in pure quantum states, J. Mod. Opt. **59**, 1525 (2012).

[75] P. J. Mosley, J. S. Lundeen, B. J. Smith, and I. A. Walmsley, Conditional preparation of single photons using parametric downconversion: A recipe for purity, New J. Phys. **10**, 093011 (2008).

[76] F. Laudenbach, H. Hübel, M. Hentschel, P. Walther, and A. Poppe, Modelling parametric down-conversion yielding spectrally pure photon pairs, Opt. Express **24**, 2712 (2016).

[77] O. Cohen, J. S. Lundeen, B. J. Smith, G. Puentes, P. J. Mosley, and I. A. Walmsley, Tailored Photon-Pair Generation in Optical Fibers, Phys. Rev. Lett. **102**, 123603 (2009).

[78] A. Clark, B. Bell, J. Fulconis, M. M. Halder, B. Cemlyn, O. Alibart, C. Xiong, W. J. Wadsworth, and J. G. Rarity, Intrinsically narrowband pair photon generation in microstructured fibres, New J. Phys. **13**, 065009 (2011).

[79] B. J. Smith, P. Mahou, O. Cohen, J. S. Lundeen, and I. A. Walmsley, Photon pair generation in birefringent optical fibers, Opt. Express **17**, 23589 (2009).

[80] T. Kim, M. Fiorentino, and F. N. C. Wong, Phase-stable source of polarization-entangled photons using a polarization Sagnac interferometer, Phys. Rev. A **73**, 012316 (2006).

[81] P. G. Evans, R. S. Bennink, W. P. Grice, T. S. Humble, and J. Schaake, Bright Source of Spectrally Uncorrelated Polarization-Entangled Photons with Nearly Single-Mode Emission, Phys. Rev. Lett. **105**, 253601 (2010).

[82] K. N. Cassemiro, K. Laiho, and C. Silberhorn, Accessing the purity of a single photon by the width of the Hong–Ou–Mandel interference, New J. Phys. **12**, 113052 (2010).

[83] C. I. Osorio, N. Sangouard, and R. T. Thew, On the purity and indistinguishability of down-converted photons, J. Phys. B **46**, 055501 (2013).

[84] See Supplemental Material at http://link.aps.org/supplemental/10.1103/PhysRevA.95.061803 for analytic calculations and for the WaveShaper transmission measurement.

[85] A. V. Smith, snlo nonlinear optics code, AS-Photonics, Albuquerque, NM .

[86] N. Montaut, L. Sansoni, E. Meyer-Scott, R. Ricken, V. Quiring, H. Herrmann, and C. Silberhorn, High efficiency plug & play source of heralded single photons, arXiv:1701.04229.

[87] D. N. Klyshko, Use of two-photon light for absolute calibration of photoelectric detectors, Sov. J. Quantum Electron. **10**, 1112 (1980).

[88] M. Avenhaus, A. Eckstein, P. J. Mosley, and C. Silberhorn, Fiber-assisted single-photon spectrograph, Opt. Lett. **34**, 2873 (2009).

[89] A. Eckstein, B. Brecht, and C. Silberhorn, A quantum pulse gate based on spectrally engineered sum frequency generation, Opt. Express **19**, 13770 (2011).